Biogeosciences Discuss., https://doi.org/10.5194/bg-2018-163
Manuscript under review for journal Biogeosciences
Discussion started: 17 April 2018

Carbonate system distribution, anthropogenic carbon and acidification in the Western Tropical South Pacific (OUTPACE 2015 transect)

Thibaut Wagener[1], Nicolas Metzl[2], Mathieu Caffin[1], Jonathan Fin[2], Sandra Helias Nuninge[1], Dominique Lefevre[1], Claire Lo Monaco[2], Gilles Rougier[1] and Thierry Moutin[1]

[1]Aix Marseille Univ, CNRS, IRD , Université de Toulon, Mediterranean Institute of Oceanography (MIO), UM 110 , 13288, Marseille, France
[2]Sorbonne Université, CNRS, IRD, MNHN, Laboratoire d'océanographie et du climat : expérimentation et approches numériques (LOCEAN), Case 100, 4 place Jussieu, 75252 Paris cedex 05, France.

Correspondence to: Thibaut Wagener (thibaut.wagener@univ-amu.fr)

Abstract.

The western tropical South Pacific was sampled along a longitudinal 4000 km transect (OUTPACE cruise, 18 Feb., 3 Apr. 2015) for measurement of carbonates parameters (total alkalinity and total inorganic carbon) between the Melanesian Archipelago (MA) and the western part of the South Pacific gyre (WGY). This manuscript reports this new dataset and derived properties: pH on the total scale (pH_T) and the $CaCO_3$ saturation state with respect to calcite (Ω_{cal}) and aragonite (Ω_{ara}). We also estimate anthropogenic carbon (C_{ANT}) distribution in the water column using the TrOCA method (Tracer combining Oxygen, inorganic Carbon and total Alkalinity). Along the OUTPACE transect, C_{ANT} inventories of 37 – 43 mol m^{-2} were estimated with higher C_{ANT} inventories in MA waters (due to a deeper penetration of C_{ANT} in the intermediate waters) than in the WGY waters although highest C_{ANT} concentrations were detected in the sub-surface waters of WGY. By combining our OUTPACE dataset with data available in GLODAPv2 (1974-2009), temporal changes in oceanic inorganic carbon were evaluated. An increase of 1.3 to 1.6 µmol kg^{-1} a^{-1} for total inorganic carbon in the upper thermocline waters is estimated whereas C_{ANT} increases of 1.1 to 1.2 µmol kg^{-1} a^{-1}. In the MA intermediate waters (27 kg m^{-3} < σ_θ < 27.2 kg m^{-3}) an increase of 0.4 µmol kg^{-1} a^{-1} of C_{ANT} is detected. Our results suggest a clear progression of ocean acidification in the western tropical South Pacific with a decrease of the oceanic pH of up to -0.0027 a^{-1} and a shoaling of the saturation depth for aragonite of up to 200 m since the pre-industrial period.

1 Introduction

Human activities inject about 10^{13} kg of carbon per year to the atmosphere which might have major consequences on climate. It is recognized that the ocean plays a key role in the control of atmospheric CO_2 through uptake by the so called "oceanic carbon pump". Through this "pump", the ocean sequesters ca. 30% of the CO_2 injected annually in the atmosphere by human activities (Le Quéré et al., 2018). A consequence of the ocean carbon uptake is a decrease of the oceanic pH (Feely

et al, 2004) which is described as ocean acidification (the so-called "other" CO_2 problem). Effects of ocean acidification have been observed on marine organisms and could affect the marine ecosystems (Riebesell et al., 2000). Improving our understanding of the oceanic CO_2 uptake relies primarily on observations of the marine carbonate cycle. Studies on the oceanic carbonate cycle have been mostly conducted in the frame of international programs. The World Ocean Circulation Experiment (WOCE) and the Joint Global Flux Study (JGOFS) in the 90's have coordinated oceanographic cruises along large sections in the ocean to collect samples through the water column and to perform accurate measurements of carbonate parameters and ancillary parameters (temperature, salinity, dissolved oxygen, nutrients,...). Since 2000, efforts have been made to "revisit" oceanic sections according to the WOCE strategy in order to assess oceanic changes at the scale of a decade. These programs have generated important databases for oceanic carbonate chemistry (e.g. GLODAP_V2 – Olsen et al., 2016).

In order to better assess the role of the ocean on the global carbon cycle, the concept of oceanic anthropogenic carbon (hereafter named C_{ANT}) has been introduced and refers to the fraction of dissolved inorganic carbon (C_T) in the ocean that originates from carbon injected by human activities in the atmosphere since the industrial revolution. As C_{ANT} is not a directly measurable quantity, it can only be estimated through assumptions that are subjected to intense scientific debate (Sabine and Tanhua, 2010). In particular, it has been recently recognized that ocean circulation changes drive significant variability in carbon uptake (De Vries et al., 2017). Detecting, separating and attributing decadal changes of the carbonates system (C_T and A_T), C_{ANT} and pH in the ocean at global or regional scales remains challenging.

Within this context, the Pacific Ocean is a particularly challenging area to study due to its size (ca. one third of the Earth's and one half of the oceanic surface). Even if, due to its remoteness from land, it remains largely under-explored by oceanographic vessels compared to other oceanic areas, the Pacific Ocean has been covered by cruises along long sections (the "P sections" from the WOCE program). Most of these sections have been revisited during the last years (see for example Sabine et al., 2008 or Kouketsu et al., 2013). In a recent study based on repeated sections in the Pacific (P16 at 150W), Carter et al (2017) observed significant increase of Cant in the top 500m around 10°S-30°S and a local carbon storage maximum around 20°S in recent years. In this context, the OUTPACE data presented in this study, associated to historical observations (since the pioneer 1974 GEOSECS) offer a new view to evaluate variability and decadal changes of C_T, C_{ANT} and pH in the tropical Pacific, here focused in the western tropical south pacific (WTSP).

The aim of this paper is to report a new dataset of oceanic inorganic carbon (based on measurements of C_T and total alkalinity (A_T)) acquired in the WTSP during the OUTPACE (Oligotrophic to UltTra oligotrophic PACific Experiment) cruise performed in 2015 (Moutin et al., 2017). The main focus of the OUTPACE cruise was to study the complex interactions between planktonic organisms and the cycle of biogenic elements on different scales, motivated by the fact that the WTSP has been identified as a hot spot of N_2 fixation (Bonnet et al., 2017). The data presented here have been partially used in another paper of the special issue (Moutin et al., 2018) in order to study the biological carbon pump in the upper (surface to 200m) water column. In this paper we will explore the carbonate data between the surface and 2000 m depth. The OUTPACE transect (Figure 1) is close to existing WOCE and GO-SHIP lines in the South Pacific : it is parallel to the zonal

P21 line (18° S visited in 1994 and 2009) and the P06 line (32° S visited in 1992, 2003 and 2010), it is crossed by the meridional P14 line (180° E visited in 1994 and 2007) and P15 line (170° W visited in 2001, 2009 and 2016) and it is situated at the eastern side of the P16 line (150° W visited in 1992, 2005 and 2014). This will allow us to compare our data with these high quality data (internally consistent through a secondary quality control (Olsen et al., 2016)) available in the Global Ocean Data analysis Project version 2 (GLODAPv2 database) and evaluate both C_T, A_T, C_{ANT} and pH_T (pH on total scale) trends in sub surface waters and at depth.

The paper is organized as follows: After describing the methods used to acquire the dataset and the way the auxiliary data have been used in Sect. 2, we briefly present the hydrographic context of the cruise in Sect. 3. We then present in Sect. 4, the carbonate dataset acquired during the cruise. In Sect. 5, estimated C_{ANT} values in the water column are presented, the validity of these estimates based on the TrOCA (Tracer combining Oxygen, inorganic Carbon and total Alkalinity) method is discussed and geographical patterns are evoked. In Sect. 6, the temporal changes in oceanic inorganic carbon in the WTSP combining data available in GLODAPv2 and our OUTPACE dataset are presented and discussed. Finally, in Sect. 7, some features in relation to ocean acidification are inferred from our dataset.

2 Material and Methods

2.1 Cruise and sampling strategy

The OUTPACE cruise took place between 18 February and 3 April 2015 from Noumea (New Caledonia) to Papeete (French Polynesia), in the WTSP on board the French research vessel “L’Atalante” (Fig. 1). A total of 18 stations were sampled mostly in the top 2000 m of the water column along a ~4000 km transect from the Melanesian archipelago to the South Pacific gyre (Moutin et al., 2017). A CTD-Rosette was deployed (1) to acquire data with CTD and associated sensors along vertical profiles and (2) to collect discrete seawater samples from 24 12-L Niskin bottles for chemical analysis. Due to technical failures on the main CTD-Rosette, for two of the casts considered in this study, a trace metal clean CTD rosette (TM-R) equipped with 24 teflon-lined GO-FLO bottles devoted to trace metal analyses was used. The configurations of both CTD Rosettes are detailed elsewhere (Moutin et al., 2017).

For carbonate parameters, seawater was sampled from 31 casts over the 18 stations. At each station, on a regular basis, samples were collected at 12 depths between the surface and 2000 m on two distinct casts: 6 samples on a 0-200 m cast and 6 samples on a 0-2000 m cast. At station SD-13, only one cast was sampled down to 500 m depth. In addition, at station LD-C, samples were collected at 24 depths on a deep cast (down to 5000 m) and 12 samples were collected at the same depth (25 m) on a “repeatability” cast. Details on the casts performed for this study are summarized in Table 1.

2.2 Chemical measurements on discrete samples

All samples were collected within less than 1 hour after arrival of the CTD rosette on deck.

Biogeosciences Discuss., https://doi.org/10.5194/bg-2018-163
Manuscript under review for journal Biogeosciences
Discussion started: 17 April 2018

2.2.1 Total alkalinity and dissolved inorganic carbon

Samples for A_T and C_T were collected in one 500 mL borosilicate glass flask (Schott Duran®) and poisoned immediately after collection with $HgCl_2$ (final concentration 20 $mg.L^{-1}$). Samples were stored at 4°C during transport and were analyzed (within 10 days) 5 months after the end of the cruise at the SNAPO-CO_2 (Service National d'Analyse des paramètres Océaniques du CO_2- LOCEAN – Paris). A_T and C_T were measured on the same sample based on a potentiometric titration in a closed-cell (Edmond, 1970). A non-linear curve fitting approach was used to estimate A_T and C_T from the recorded titration data (Dickson 1981, DOE 1994). Measurements were calibrated with Certified Reference Material (CRM) provided by Dr. A Dickson, Univ. Southern California (Batch 139 - C_T : 2023.23 ± 0.70 µmol kg^{-1} and A_T: 2250.82 ± 0.60 µmol kg^{-1}, see Dickson, 2010). The reproducibility, expressed as the standard deviation of the CRM analysis (n=15), was 4.6 µmol kg^{-1} for A_T and 4.7 µmol kg^{-1} for C_T . Based on replicate measurements at station LD-C (cast out_c_194, see Table 1) the reproducibility, expressed as the standard deviation of the analysis of the replicates collected at the same depth (ca. 25 m, n=12) from different Niskin bottles was 3.6 µmol kg^{-1} for A_T (average value = 2324.7 µmol kg^{-1}) and 3.7 µmol kg^{-1} for C_T (average value = 1969.7 µmol kg^{-1}).

2.2.2 Oxygen concentration

Dissolved oxygen concentration [O_2] was measured following the Winkler method (Winkler, 1888) with potentiometric endpoint detection (Oudot et al., 1988). For sampling, reagents preparation and analysis, the recommendations from Langdon (2010) were carefully followed. The thiosulfate solution was calibrated by titrating it against a potassium iodate certified standard solution of 0.0100N (CSK standard solution – *WAKO*). The reproducibility, expressed as the standard deviation of replicates samples was 0.8 µmol kg^{-1} (n=15, average value= 195.4 µmol kg^{-1}).

2.3 Vertical profiles of hydrological and biogeochemical parameters

2.3.1 CTD measurements

CTD measurements were ensured by a Seabird™ 911+ underwater unit which interfaced an internal pressure sensor, two redundant external temperature probe (SBE3plus) and two redundant external conductivity cells (SBE4C). The sensors were calibrated pre- and post-cruise by the manufacturer. No significant drift between the redundant sensors was observed. For vertical profiles, full resolution data (24 Hz) were reduced to 1 dbar binned vertical profiles on the downcast with a suite of processing modules using the Seabird™ dedicated software (*SbeDataProcessing*). For values at the closure of the Niskin bottles, values collected at 24 Hz were averaged 3 s before and 5 s after closure of the bottle. In this study, for temperature and conductivity the signal of the first sensors has been systemically used. For the two TM-R casts, no significant difference with the main CTD-Rosette on temperature and conductivity was observed.

Biogeosciences Discuss., https://doi.org/10.5194/bg-2018-163
Manuscript under review for journal Biogeosciences
Discussion started: 17 April 2018

2.3.2 Oxygen measurements

[O_2] was also measured with a SBE43 electrochemical sensor interfaced with the CTD unit. The raw voltage was converted to oxygen concentration with 13 calibration coefficients based on the Seabird™ methodology derived from Owens and Millard (1985). Three of these coefficients (the oxygen signal slope, the voltage at zero oxygen signal, the pressure correction factor) were adjusted with the concentrations estimated with the Winkler method on samples collected at the closure of the bottles. One unique set of calibration coefficients has been applied to all oxygen profiles from the cruise because no significant drift of the sensor was observed during the time of the cruise. For the two TM-R casts, values have been corrected with a drift and offset based on the comparison of 15 pairs of casts (main CTD-rosette / TM-R) collected close in time (less than 2 h) and space (less than 1 nautical mile) over the entire OUTPACE transect.

2.4 Derived parameters

Practical salinity (S_P) was derived from conductivity, temperature and pressure with the EPS-78 algorithm. Absolute salinity (S_A), potential temperature (θ), conservative temperature (Θ) and potential density (σ_θ) were derived from Sp, temperature, pressure and the geographic position with the TEOS-10 algorithms (Valdarez et al., 2011). This five derived parameters were calculated within the processing with *Seabird*™ dedicated software.

Seawater pH on the total scale (pH_T) and the $CaCO_3$ saturation state with respect to calcite (Ω_{cal}) and aragonite (Ω_{ara}) were derived from A_T and C_T with the "Seacarb" R package (Gattuso and Lavigne, 2009). Following the recommendations from Dickson et al. (2007), the constants for carbonic acid K_1 and K_2 from Lueker et al. (2000), the constant for hydrogen fluoride K_F from Perez and Fraga (1987) and the constant for hydrogen sulfate K_S from Dickson (1990) were used. Orthophosphate and silicate concentration were considered in the calculation. Methods for nutrients measurement are presented in details in Fumenia et al. (2018). When nutrient data were not available (Station SD-8), silicate and orthophosphate were estimated from the nutrient profile measured on cast out_c_163 (interpolated values). Apparent Oxygen Utilization (AOU) was computed from the difference between oxygen solubility (at p=0 dbar, θ and S_P) estimated with the "Benson and Krause coefficients" in Garcia and Gordon (1992) and in situ [O_2].

For estimation of C_{ANT}, the TrOCA method was used. The TrOCA approach was first proposed in Touratier and Goyet (2004a, b) with improvements in Touratier et al. (2007). In brief, the TrOCA parameter is defined as a combination of A_T, C_T and [O_2] that accounts for biologically induced relative changes among these parameters (with constant stoichiometric ratios). TrOCA is thus a quasi-conservative tracer derived from C_T in the ocean. Within a defined water mass, changes in TrOCA over time are independent from biology and can be attributed to the penetration of C_{ANT}. In consequence C_{ANT} can be calculated in a parcel of water from the difference between current and pre-industrial TrOCA (TrOCA°) divided by a stoichiometric coefficient. The simplicity of the TrOCA method relies on the fact that a simple formulation for TROCA° has been proposed based on potential temperature and alkalinity and thus an estimation of C_{ANT} can be done by a simple

calculation using C_T, A_T, $[O_2]$ and θ. In this study, the formulation proposed in eq. 11 in Touratier et al. (2007) is used to calculate C_{ANT} and is reminded here in Eq. (1).

$$C_{ANT} = \frac{[0_2] + 1.279\left(C_T - \frac{A_T}{2}\right) - \exp\left(7.511 - 1.087.10^{-2}\theta - \frac{7.81.10^{-5}}{A_T^2}\right)}{1.279} \quad (1)$$

This formulation is based on an adjustment of the TrOCA coefficients using $\Delta^{14}C$ and CFC-11 from the GLODAP-V1 database (Key et al., 2014). Touratier et al. (2007) estimated the overall uncertainty of the C_{ANT} with TrOCA method to 6 µmol kg^{-1}.

2.5 Data from available databases

For comparison with existing values of carbonate chemistry in the area of the OUTPACE cruise, relevant data were extracted from GLODAPv2 database (NDP-93 - Olsen et al. 2016). The specific data file for the Pacific Ocean was used (downloaded from https://www.nodc.noaa.gov/ocads/oceans/GLODAPv2/ on December 14, 2017). For comparison with OUTPACE data, GLODAPv2 data were selected between 22°S and 17°S and between 159°E and 159° W (going westwards). For specific comparisons in the Melanesian archipelago (MA) and the South Pacific Western Gyre waters (WGY) a zonal subset of the extracted data was used: 159°E and 178° W for MA and 170°W to 159°W for WGY (see Fig. 1).

3 Hydrological context along the OUTPACE transect

The hydrological context encountered during the OUTPACE transect is presented with a Θ – S_A diagram between 0 and 2000 dbar on Fig. 2. A detailed description of the water masses encountered during the OUTPACE cruise can be found in Fumenia et al. (2018). Briefly, from the surface to 2000 dbar, the following features are distinguished: the surface waters ($\sigma_\theta < 23.5$) were characterized by temperatures over 25 °C with increasing temperature and salinity towards the east and AOU close to zero. Under the the surface water, the upper thermocline waters (UTW) presented a maximum in salinity reaching values higher than 36 g kg^{-1} in the eastern part of the cruise. In the lower thermocline waters, S_A decreased with depth with a more pronounced decrease in the eastern part than in the western part whereas AOU is higher in the eastern part than in the western part of the studied area. These differences in lower thermocline waters have been described for South Pacific Central Waters (SPCW) with more saline western (WSPCW) and less saline eastern (ESPCW) waters (Tomczack and Godfrey, 2001). Below the thermocline, intermediate waters are constituted of Sub-Antarctic Mode Waters (SAMW) and Antarctic Intermediate Waters (AAIW). AAIW have a salinity minimum close to the $\sigma_\theta = 27$ kg m^{-3} isopycnal . Hartin et al. (2011) defines SAMW with σ_θ values between 26.80 and 27.06 kg m^{-3}, and AAIW with σ_θ values between 27.06 and 27.40 kg m^{-3}. The separation of both waters is not trivial in the subtropical area. SAMW is generally associated to lower AOU than AAIW. Finally deep waters constituted of Upper Circumpolar Deep Waters (UCDW) correspond to an increase in salinity and AOU for depth corresponding to $\sigma_\theta > 27.4$ kg m^{-3}.

Biogeosciences Discuss., https://doi.org/10.5194/bg-2018-163
Manuscript under review for journal Biogeosciences
Discussion started: 17 April 2018

In this study, discussion will sometimes make distinction between two sub-regions along the OUTPACE transect: MA and WGY (See Sect. 2.5 for definition). This distinction is mainly based on geographic and oceanographic arguments. Indeed, these two sub-regions are geographically separated by the Tonga volcanic arc. WGY is characterized by higher surface temperature and a higher salinity in the upper thermocline waters than MA. The difference between these sub-regions is evidenced by the difference in oligotrophy (Moutin et al., 2018). Due to specific conditions in the transition area between the MA and WGY (de Verneil et al., 2017), SD11, SD12 and LDB were discarded from both groups in this study following the arguments in Moutin et al. (2018).

4 Carbonate chemistry along the OUTPACE transect

A_T and C_T measured along the OUTPACE transect are presented on Fig 3a and 3b. All vertical profiles for A_T, A_T normalized to S_A = 35 g kg^{-1} ($A_{T\,n35}$) and C_T are presented on Fig. 3e, 3f and 3G. A_T ranged between 2300 and 2400 µmol.kg^{-1}. Below the surface, a pronounced maximum in A_T was observed associated to the saltier upper thermocline waters. When normalized to S_A = 35 g kg^{-1}, A_T values are remarkably constant in the upper 500 dbar with values between 2270 and 2310 µmol kg^{-1}. Below 500 dbar, A_T increases with depth up to ca. 2400 µmol kg^{-1} indicating that alkalinity changes are mostly due to salinity changes in the upper water column whereas the increase in the deep waters is mainly due to carbonate biominerals remineralization. C_T values are close to 1950 µmol kg^{-1} in the surface and increase with depth up to 2300 µmol kg^{-1} at 2000 dbar. The C_T gradient in the upper water column has been described in Moutin et al. (2008). Below 2000 dbar, C_T is relatively invariant with slightly lower values in the bottom waters. A_T and C_T values in deep waters measured during OUTPACE are in good agreement with the data of the GLODAPv2 database (Fig. 3E, 3f et 3g). No systematic adjustment of the OUTPACE dataset with the GLODAPv2 dataset was performed because only very few data are available in the deep ocean where crossover comparison can be performed for cruises carried out in different decades. Nevertheless, for the only "deep" cast performed during OUTPACE (out_c_163 at station C), we performed a simple crossover analysis with the station 189 (located at 107 km kilometers from OUTPACE station C) of the Japanese "P21 revisited" cruise in 2009. We compared interpolated profiles on density surfaces values ($27.75 < \sigma_\theta < 27.83$ corresponding to pressure levels of ca. 3000 to 5500 dbar) . The estimated offsets are -2.0 ± 4.2 µmol kg^{-1} for A_T and -2.0 ± 4.4 µmol kg^{-1} for C_T lies within the repeatability of method (see Sect. 2). This simple quality control procedure seems to indicate that no systematic adjustment is needed.

Derived parameters from the A_T and C_T measurements are presented on Fig. 3c for pH_T values (estimated at in situ temperature and pressure). pH_T decreases from values close to 8.06 in surface to values close to 7.84 at 2000 m. Surface values of pH are typical of subtropical warm waters and are in a similar range as the austral summer values estimated by Takahashi et al. (2014) in this area (8.06 - 8.08). Figure 3d represents the vertical distribution of computed values of Ω_{ara} along the OUTPACE transect. Seawater is supersaturated with respect to aragonite ($\Omega_{ara}>1$) at surface with Ω_{ara} values of ca. 4.0 again in good agreement with the austral summer values of 4 – 4.4 estimated by Takahashi et al. (2014) in this area. Values of Ω_{ara} decrease with depth and seawater becomes undersaturated with respect to aragonite ($\Omega_{ara}<1$) at an horizon

situated below 1000 dbar in the west and above 1000 dbar in the eastern part of the cruise, with a general shoaling of the Ω_{ara} values from west to east, in good agreement with a previous study by Murata et al. (2015) in this area. As expected, values for Ω_{cal} show the overall same pattern as Ω_{ara} with the important difference that seawater up to 2000 dbar was supersaturated with respect to calcite ($\Omega_{cal}>1$) (data not shown). At the deep cast, seawater becomes undersaturated with respect to calcite ($\Omega_{cal}<1$) at an horizon situated below 3000 dbar.

5 Anthropogenic carbon estimation along the OUTPACE transect

The TrOCA method is a way to quantify C_{ANT} in the ocean based on C_T, A_T, $[O_2]$ and θ. This method has been used and compared to other methods in different oceanic areas (e.g. Lo Monaco et al., 2005; Alvarez et al., 2009; Vazquez-Rodriguez et al.,2009) : based on specific C_{ANT} inventories in the water column, the TrOCA method reasonably agreed with the other methods (including transient tracer based method). However, Yool et al. (2009) "tested" the TrOCA method within an ocean general circulation model and argued that the use of globally uniform parametrization for the estimation of the preindustrial TrOCA is a source of significant errors but also that even with regionally "tunned" parameters a global bias in the method exists. As no tracers of water mass age were measured during the OUTPACE cruise, the main motivation for using the TrOCA method was to make C_{ANT} estimations based on a simple calculation from parameters acquired within the cruise as done in other cruises conducted in south tropical Pacific waters (e.g. Azouzi et al., 2009; Ganachaud et al., 2017).

As mentioned by Touratier et al. (2007), C_{ANT} estimates cannot be considered within the mixed layer because the underlying hypotheses used in the formulation of TrOCA may not be verified due to biological activity and gas transfers across the air–sea interface. To avoid this issue, C_{ANT} estimates are generally used below the "permanent" mixed layer depth (e.g. Alvarez et al., 2009, Carter et al., 2017). For the OUTPACE area, Moutin et al. (2018) shows that the mixed layer depth do not exceed 70 m in the area. Even if the depth of the deep chlorophyll maximum was encountered below 100 dbar along the transect, we will consider C_{ANT} values up to 100 dbar. It can be mentioned that the C_{ANT} values of 50-60 µmol kg^{-1} in the top of the water column (100 dbar), are in reasonable agreement with a rough estimate of thermodynamic consistent C_T changes: by assuming that CO_2 in surface seawater is in equilibrium with the atmosphere, we estimated that with a partial pressure of CO_2 (pCO_2) of 280 µatm at the pre-industrial period, a pCO_2 of 380 µatm during OUTPACE (Moutin et al., 2018) and a constant A_T over time of 2300 µmol kg^{-1}, C_T change in surface waters between pre-industrial and 2015 is of ca. 65 µmol kg-1 for a temperature of surface waters between 25 and 28 °C. For OUTPACE, C_{ANT} estimates below 1000 dbar, were not significantly different from 0 µmol kg^{-1} with a standard deviation of 6.3 µmol kg^{-1}, in the range of the error estimate.

C_{ANT} distribution along the OUTPACE transect is presented on Fig. 4a and all vertical profiles for C_{ANT} are presented on Fig. 4b with a more detailed view of the first 1500 dbar of the water column on Fig. 4c. Figures 4b and 4c distinguish values from the MA and the WGY area. The C_{ANT} vertical profiles suggest a penetration of anthropogenic carbon up to 1000 dbar. As mentioned before, estimated values of C_{ANT} reach values of 60 µmol kg^{-1} at depth of 100 dbar, then regularly decreases to values close to 10 - 20 µmol kg^{-1} at a depth of 1000 dbar and reaches values close to 0 µmol kg^{-1} below 1500 dbar. The zonal

C_{ANT} section along the OUTPACE transect (Fig. 4a) presents two singularities: (1) a deeper penetration of C_{ANT} in the western part of the transect with values of C_{ANT} reaching 40 µmol kg^{-1} around the isopycnal layer of 27 kg m^{-3} (ca. 700 dbar) with a coherent behavior with the distribution of AOU and (2) a larger accumulation of C_{ANT} in the eastern part of the transect centered around the isopycnal layer of 25 kg m^{-3} (ca. 200 dbar). This singularity in the distribution of C_{ANT} is reflected in the estimated inventories in the 0 - 1000 dbar water ($C_{ANT}INV_{1000}$) and 0- 2000 dbar ($C_{ANT}INV_{2000}$) water column presented on Table 2 : for stations in the MA area $C_{ANT}INV_{1000}$ represents between 82% and 90% of the $C_{ANT}INV_{2000}$, whereas it represents more than 90% in the WGY area indicating a lower penetration depth of C_{ANT} in the eastern part of the cruise.

Several studies have identified deeper C_{ANT} penetration in the Western South Pacific than in the Eastern South Pacific at tropical and subtropical latitudes. The primary reason for this longitudinal difference might be associated to deeper convection in the western part and upwelling in the eastern part. AAIW has been described as the lower limit of the penetration of C_{ANT} in the ocean interior of the South Pacific (Sabine et al., 2004). Moreover, a recent study by deVries et al., (2017) shows that ocean circulation variability is the primary driver for changes in oceanic CO_2 uptake at decadal scales. Based on C_T changes between the two repeated visits of the longitudinal P21 line (18° S close to the OUTPACE transect) in 1994 and 2009, Kouketsu et al. (2013) shows faster increase of C_{ANT} in the western part than in the eastern part of the section. They also postulate that C_{ANT} may have been transported by deep circulation associated to the AAIW. In the subtropical Pacific along the P06 line (longitudinal section at ca. 32°S), Murata et al. (2007), also identified an increase of C_{ANT} in the SAMW and AAIW. Waters et al. (2011), based on the extended multiple linear regression (eMLR) method along the P06 line (and taking into account a third visit) attributes the deeper penetration of C_{ANT} in the western part of the section to the local formation of subtropical mode water in the area.

In the eastern part of the OUTPACE cruise, the detected accumulation of C_{ANT} in the upper thermocline waters may be related to recent observations of a significant accumulation of C_{ANT} at latitudes around 20°S on the P16 meridional transect along 150°W by Carter et al. (2017). This change in C_{ANT} accumulation is attributed to changes in the degree of the water mass ventilation due to variability in southern Pacific subtropical cell. Along the P16 line, Carter et al. (2017) observed high values of C_{ANT} (up to 60 µmol.kg^{-1}) for the upper water column at the latitude of OUTPACE area in good agreement with our estimates in WGY in the upper water column. It should also be mentioned that, due to the presence of one of the main OMZ area, denitrification occurs in the eastern South Pacific and can be traced by the N* parameter (Gruber and Sarminento, 2007). Denitrification, by transforming organic carbon to inorganic carbon without consumption of oxygen, could induce an overestimation of C_{ANT} by the TrOCA method (and other back calculation methods). Horizontal advection by the south equatorial current of the strong negative N* signal originating from the Eastern Pacific towards the western Pacific was previously described (Yoshikawa et al., 2015). Fumenia et al. (2008) have estimated N* along the OUTPACE transect and show slightly negative N* values in the upper thermocline waters at the eastern side of the OUTPACE transect where the highest C_{ANT} values are estimated.

Finally, if we consider that all C_{ANT} is distributed in the upper 2000 dbar of the water column, our $C_{ANT}INV_{2000}$ of 43 ± 4 mol m^{-2} for MA and 37.3 ± 0.4 mol m^{-2} for WGY (Table 2) can be considered as water column C_{ANT} inventories. The C_{ANT} is

signigicantly higher in MA than in WGY. The C_{ANT} concentrations during OUTPACE are about twice the C_{ANT} estimated in 1994 (P21 line, Sabine et al., 2002; their Fig. 5) leading to a doubling of C_{ANT} inventory, from about 20 mol m^{-2} in 1994 to 40 mol m^{-2} in 2015. Sabine et al., (2008) estimated a column inventory change of 0.5 mol m^{-2} a^{-1} for the years 2000 and Carter et al. (2007) estimated a recent year column inventory change of up to 0.8 mol m^{-2} a^{-1} at 20°S along the P16 line (170°W). When adding the C_{ANT} inventories of the early 90s to the changes in inventories of the recent years, our inventories $C_{ANT}INV_{2000}$ are slightly higher but in reasonable agreement. Our results are also in the range of C_{ANT} inventory evaluated around 40 - 50 mol m^{-2} in this region for a reference year 2010 (Khatiwala et al., 2013).

6 Temporal changes of inorganic carbon in the OUTPACE area

Based on the available GLODAPv2 data, temporal changes in the OUTPACE area have been assessed (Fig. 5 and Table 3). The variation of oceanic parameters with time are estimated on two isopycnal layers : A layer with 25 kg m^{-3} < σ_θ < 25,5 kg m^{-3} (hereafter named $\sigma_{\theta\,25}$) and a layer with 27 kg m^{-3} < σ_θ < 27.2 kg m^{-3} (hereafter named $\sigma_{\theta\,27}$). These two layers correspond to the singularities in C_{ANT} discussed in the former section. $\sigma_{\theta\,25}$ can be considered as characteristic of the upper thermocline waters (core of the salinity maximum, Fig 2) whereas $\sigma_{\theta\,27}$ can be considered as characteristic of intermediate waters of southern origin (core of the salinity minimum). All the values associated to these two layers are spread between 145 and 301 dbar for $\sigma_{\theta\,25}$ and between 571 and 896 dbar for $\sigma_{\theta\,27}$.

Temporal variations of C_T and C_{ANT} between 1970 and 2015 are presented on Fig 5. The observed temporal variations for A_T, $[O_2]$, C_T and C_{ANT} were adjusted to a linear model to check for significant trends on data collected between 1980 and 2015 (OUTPACE cruise). The results of the performed regression analyses are presented on table 2. Values from the MA and the WGY area distinguished. Even if presented on Figure 5, data collected before 1980 from the GLODAPv2 database are disregarded in the estimation of the temporal trends. Indeed, for the OUTPACE area, data prior to 1980 originate from one single GEOSEC cruise in 1974, with only one measured point for $\sigma_{\theta\,27}$ at WGY and no points at $\sigma_{\theta\,25}$ for WGY and WMA.

At $\sigma_{\theta\,25}$, a significant decrease of A_T of -0.2 µmol $kg^{-1}.a^{-1}$ is observed over the entire OUTPACE area. A decrease of - 0.2 µmol.$kg^{-1}.a^{-1}$ is also observed in MA area, whereas no significant trend is observed for the WGY area. However, when A_T is normalized to salinity, no significant trends are observed in $A_{T\,n35}$. No significant trend are observed for $[O_2]$. Significant trends over the entire area (+ 1.3 µmol kg^{-1} a^{-1}), in MA (+ 1.4 µmol kg^{-1} a^{-1}) and in WGY (+ 1.6 µmol kg^{-1} a^{-1}) are observed for C_T. For C_{ANT}, the trends are slightly slower (+ 1.1 to 1.2 µmol kg^{-1} a^{-1}) and not significantly different between MA and WGY. If we assume a C_T increase of 1 µmol kg^{-1} a^{-1} associated to the recent rise in atmospheric CO_2 (see for example Murata et al., 2007), the C_T increase in the OUTPACE area is faster than thermodynamics would govern whereas the C_{ANT} is close to this thermodynamic value. Such an “over accumulation” has been observed by Carter et al. (2017) at 20°S on the P16 line on C_{ANT} changes estimated between 2005 and 2015. No significant differences are observed in the trend of C_{ANT} between MA and WGY. This suggests that even if the higher levels of C_{ANT} observed at $\sigma_{\theta\,25}$ in WGY (see former section) than in MA would be related to denitrification, they are not associated to a faster accumulation rates of C_{ANT} induced by changes in

denitritification. Indeed, Murata et al. (2007) showed that based on a direct relation between C_T and N*, the influence of denitrification should be negligible on C_{ANT} accumulation rates in this area. The small estimated change in A_T (less than - 3 µmol kg^{-1} per decade) which could indicate some changes in remineralization processes has a very low impact on TrOCA° used in the estimation of C_{ANT} and cannot explain the difference of C_{ANT} between MA and WGY observed in the upper thermocline waters.

At $\sigma_{\theta 27}$, the only significant trend observed is an increase in C_{ANT} of ca. 0.4 µmol.kg^{-1}.a^{-1} in the MA area. This trend is compatible with the observed increase of C_{ANT} by Kouketsu et al. (2013) along the P21 line close to the isopycnal layer 27 kg m^{-3}. As this increase is not observed in WGY and if we assume that the $\sigma_{\theta 27}$ is filed with AAIW waters, this suggest that the accumulation of C_{ANT} in AAIW is faster west of 170°W line than to the east, but no clear explanation for this trend can be given.

7 Towards an enhanced "Ocean Acidification" in the WTSP?

Temporal variations of pH_T between 1970 and 2015 is presented on Fig. 5c and 5f with rates of pH_T decrease of -0.0022 ± 0.0004 a^{-1} for MA and -0.0027 ± 0.0004 a^{-1} for WGY at $\sigma_{\theta 25}$ (Table 3) between 1980 and 2015. Based on the C_{ANT} rates estimated in the previous section (1.1 to 1.2 µmol kg^{-1} a^{-1}), and based on a constant value of A_T of 2285 µmol kg^{-1} (mean value of A_{Tn35} on $\sigma_{\theta 25}$) and a temperature of 20°C, we can estimate a pH_T decrease rate of -0.0023 to -0.0025 a^{-1}. This indicates that rates of oceanic pH decrease (ocean acidification) can mostly be explained by the increase of C_{ANT}. These rates of acidification are higher than the values reported by Waters et al. (2011) in the Western South Pacific along the P06 Line (south of OUTPACE area at 32°S) between two visits in 1992 and 2008. They are also higher than the surface rates of pH decrease of –0.0016 ± 0.0001 a^{-1} recorded at the HOT time-series station in the tropical North Pacific and of –0.0017 ± 0.0001 a^{-1} and –0.0018 ± 0.0001a^{-1} in the tropical North Atlantic at BATS and ESTOC stations respectively (Bates et al., 2014). However, our results in subsurface ($\sigma_{\theta 25}$) based on GLODAPv2 and OUTPACE data (C_T and A_T), can be compared with pH trends derived from fCO2 surface observations (e.g. Lauvset et al, 2015). In the southern subtropical and equatorial Pacific regions, using SOCAT version 2, Lauvset et al. (2015) evaluate contrasting fCO2 and pH trends, ranging between +1.1 µatm a^{-1} and +3.5 µatm a^{-1} for fCO2 and between -0.001 a^{-1} and -0.0023 a^{-1} for pH. If we revisit these estimates, using surface fCO2 observations available in the OUTPACE region (18-22°S/170-200°E) in SOCAT version 5 (Bakker et al., 2016; www.socat.info) and assuming a constant alkalinity (2300 µmol/kg, average of surface data), we can calculate pH_T and C_T from fCO2 and temperature data. The resulting long-term trends for the period 1980-2016 for fCO2, C_T and pH_T are respectively +1.3 µatm a^{-1}, +1 µmol kg^{-1} a^{-1} and -0.0013 a^{-1}. Interestingly for the period 2000-2016 the trends are +2.6 µatm a^{-1}, +2 µmol kg^{-1} a^{-1} and -0.0025 a^{-1}, suggesting an acceleration of the signals in recent years. These results based on fCO2 observations in surface waters, confirm the trends we detected for C_T and pH_T in subsurface layers ($\sigma_{\theta 25}$).

On Fig. 6, estimates of the so-called "Anthropogenic pH change" ($\Delta^{ANT}pH_T$) and "Anthropogenic Ω_{ara} change" ($\Delta^{ANT}\Omega_{ara}$) which corresponds to the difference of pH and Ω_{ara} between the time of the OUTPACE cruise (modern time) and the pre-

industrial period are presented. The pH and Ω_{ara} correspond to the values presented on Fig. 3, whereas the pre-industrial values corresponds to pH and Ω_{ara} estimated with C_T minus C_{ANT}. All other parameters (temperature, salinity, alkalinity and nutrients) are assumed to remain constant over time. The main features for the distribution of $\Delta^{ANT}pH_T$ and $\Delta^{ANT}\Omega_{ara}$ logically reflect the distribution of the estimated C_{ANT} in this study because C_{ANT} is the only driving force in these estimations. The estimated pH_T decrease reaches values slightly higher than 0.1 and the estimated Ω_{ara} decrease reaches values of 0.75 since the pre-industrial period for areas with the highest C_{ANT} accumulation. When considering an error on C_{ANT} of 6 µmol kg^{-1}, we can assume that we are able to distinguish changes of 0.0012 for pH and 0.06 for Ω_{ara}. Decreases of pH_T and Ω_{ara} are thus detectable below 1000 dbar in the MA waters and above 1000 dbar in WGY waters.

A decrease of pH_T of ~0.1 units since the pre-industrial period is a generally accepted value for oceanic waters affected by C_{ANT} penetration (see e.g. Raven et al., 2005). Several studies have assessed the rate of ocean acidification based on successive visits to different oceanic areas. For the South Pacific Ocean, Carter et al. (2017) reports decreases of oceanic pH_T since the pre-industrial period of -0.09 and -0.11 pH units for the latitude band from 10 to 20°S and from 20 to 30°S, respectively, along the P16 line (150°W) situated on the eastern side of the OUTPACE area. These are in good agreement with our estimates in this area.

Decreases of Ω_{ara} in the WTSP have been discussed in detail along the P21 line by Murata et al. (2015). Based on mean values in the upper water column (< 400 dbar) in regions defined by specific features in the dataset, a decrease of Ω_{ara} at a rate of 0.017 a^{-1} is observed for the western part of the OUTPACE area whereas a much smaller decrease of 0.005 a^{-1} is estimated for the eastern part of the OUTPACE area. This important difference between the western and the eastern part of the OUTPACE area are not observed in our analysis. Based on an interpolation of the estimated Ω_{ara} during OUTPACE and the pre-industrial $\Omega_{ara,}$, we calculated the depth of the horizon where $\Omega_{ara} = 1$ for the different stations of the OUTPACE transect (Table 2) in 2015 and the pre-industrial period base on the $\Delta^{ANT}\Omega_{ara}$ estimates. We observed an upward migration of aragonite saturation horizon of up to 220 m in the MA area along the OUTPACE transect (Table 2 and Fig 6c). These upward migration of the $\Omega_{ara} = 1$ horizon is higher than the migration observed in early studies (Feely et al. 2004) in the South Equatorial Pacific based on the WOCE dataset illustrating the continuous acidification of the WTSP.

8 Conclusion

Based on $A_{T,}$ and C_T data and related properties collected during the OUTPACE cruise, we estimated different parameters of the carbonate system along a longitudinal section of nearly 4000 km and up to 2000 dbar in WTSP. Even if the vertical and horizontal resolution is low compared to the WOCE lines and precludes a rigorous comparison with this high quality dataset, we estimated that the measured carbonate chemistry parameters are in good agreement with previous data collected in this area. Based on estimation of C_{ANT} from the TrOCA method, we find C_{ANT} penetration in the WTSP and impacts on pH and saturation state of calcium carbonate since the pre-industrial period that are in good agreement with previous observation in this area. Our estimates of C_{ANT} inventories are confirming a recent increase of C_{ANT} accumulation in the WTSP. As

mentioned above, C_{ANT} from TrOCA estimates are not reliable in surface layer. However, based on GLODAPv2 and SOCAT database, our estimation of C_{ANT} in sub surface seems to be in good agreement with expected changes in surface waters. We therefore extended to the surface, our estimates of C_{ANT} at 100 dbar in order compute C_{ANT} Inventories in the water column. Even if other parameters needs to be considered, Fig. 6c illustrates the link between accumulation of C_{ANT} in the water column and ocean acidification along the OUTPACE transect. The enhanced impact of ocean acidification in the Subtropical South Pacific suggested by our study highlight the necessity of sustained research efforts in this largely under-explored part of the World Ocean. The presented dataset collected along the OUTPACE transect could complement existing section visited nearly every decade in the South Pacific ocean and in particular the P21 line which was last visited in 2009.

Acknowledgements

This is a contribution of the OUTPACE (Oligotrophy from Ultra-oligoTrophy PACific Experiment) project (https://outpace.mio.univ-amu.fr/) funded by the French research national agency (ANR-14-CE01-0007-01), the LEFE-CyBER program (CNRS-INSU), the GOPS program (IRD) and the CNES (BC T23, ZBC 4500048836). The OUTPACE cruise (http://dx.doi.org/10.17600/15000900) was managed by the MIO (OSU Institut Pytheas, AMU) from Marseille (France) which has received funding from European FEDER Fund under project 1166-39417. All data and metadata are available at the following web address: http://www.obs-vlfr.fr/proof/php/outpace/outpace.php. SNAPO-CO2 service at LOCEAN is supported by CNRS-INSU and OSU Ecce-Terra. The authors thank the crew of the R/V L'Atalante for outstanding shipboard operation. Catherine Schmechtig is warmly thanked for the LEFE CYBER database management. Aurelia Lozingot is acknowledged for the administrative work. Pierre Marrec is thanked for his insightful comments on the present work.

References

Álvarez, M., Lo Monaco, C., Tanhua, T., Yool, A., Oschlies, A., Bullister, J. L., Goyet, C., Metzl, N., Touratier, F., McDonagh, E., and Bryden, H. L.: Estimating the storage of anthropogenic carbon in the subtropical Indian Ocean: a comparison of five different approaches, Biogeosciences, 6, 681-703, https://doi.org/10.5194/bg-6-681-2009, 2009.

Azouzi, L., et al.,: Corrigendum to "Anthropogenic carbon distribution in the eastern South Pacific Ocean" published in Biogeosciences, 6, 149–156, 2009, Biogeosciences, 6, 361-361, https://doi.org/10.5194/bg-6-361-2009, 2009.

Bakker, D. C. E., Pfeil, B., Landa, C. S., Metzl, N., O'Brien, K. M., Olsen, A., Smith, K., Cosca, C., Harasawa, S., Jones, S. D., Nakaoka, S.-I., Nojiri, Y., Schuster, U., Steinhoff, T., Sweeney, C., Takahashi, T., Tilbrook, B., Wada, C., Wanninkhof, R., Alin, S. R., Balestrini, C. F., Barbero, L., Bates, N. R., Bianchi, A. A., Bonou, F., Boutin, J., Bozec, Y., Burger, E. F., Cai, W.-J., Castle, R. D., Chen, L., Chierici, M., Currie, K., Evans, W., Featherstone, C., Feely, R. A., Fransson, A., Goyet, C., Greenwood, N., Gregor, L., Hankin, S., Hardman-Mountford, N. J., Harlay, J., Hauck, J., Hoppema, M., Humphreys, M. P., Hunt, C. W., Huss, B., Ibánhez, J. S. P., Johannessen, T., Keeling, R., Kitidis, V., Körtzinger, A., Kozyr, A., Krasakopoulou, E., Kuwata, A., Landschützer, P., Lauvset, S. K., Lefèvre, N., Lo Monaco, C., Manke, A., Mathis, J. T., Merlivat, L., Millero,

F. J., Monteiro, P. M. S., Munro, D. R., Murata, A., Newberger, T., Omar, A. M., Ono, T., Paterson, K., Pearce, D., Pierrot, D., Robbins, L. L., Saito, S., Salisbury, J., Schlitzer, R., Schneider, B., Schweitzer, R., Sieger, R., Skjelvan,acceleration anglais I., Sullivan, K. F., Sutherland, S. C., Sutton, A. J., Tadokoro, K., Telszewski, M., Tuma, M., Van Heuven, S. M. A. C., Vandemark, D., Ward, B., Watson, A. J., and Xu, S.: A multi-decade record of high-quality fCO_2 data in version 3 of the Surface Ocean CO_2 Atlas (SOCAT), Earth Syst. Sci. Data, 8, 383-413, doi:10.5194/essd-8-383-2016, 2016

Bates, N.R., Astor, Y.M., Church, M.J., Currie, K., Dore, J.E., González-Dávila, M., Lorenzoni, L., Muller-Karger, F., Olafsson, J. and Santana-Casiano, J.M.: A time-series view of changing ocean chemistry due to ocean uptake of anthropogenic CO_2 and ocean acidification. Oceanography 27(1):126–141, doi: 10.5670/oceanog.2014.16, 2014.

Bonnet, S., Caffin, M., Berthelot, H. and Moutin, T.: Hot spot of N 2 fixation in the western tropical South Pacific pleads for a spatial decoupling between N 2 fixation and denitrification, Proc. Natl. Acad. Sci., 114(14), E2800–E2801, doi:10.1073/pnas.1619514114, 2017.

Carter, B. R., et al.: Two decades of Pacific anthropogenic carbon storage and ocean acidification along Global Ocean Ship-based Hydrographic Investigations Program sections P16 and P02, Global Biogeochem. Cycles, 31, 306–327, doi:10.1002/2016GB005485, 2017.

de Verneil, A., Rousselet, L., Doglioli, A. M., Petrenko, A. A., and Moutin, T.: The fate of a southwest Pacific bloom: gauging the impact of submesoscale vs. mesoscale circulation on biological gradients in the subtropics, Biogeosciences, 14, 3471-3486, https://doi.org/10.5194/bg-14-3471-2017, 2017.

DeVries, T., Holzer, M., and Primeau, F.: Recent increase in oceanic carbon uptake driven by weaker upper-ocean overturning. Nature 542, 215-218. doi:10.1038/nature21068, 2017

Dickson, A. G.: An exact definition of total alkalinity and a procedure for the estimation of alkalinity and total inorganic carbon from titration data. Deep-Sea Res. 28A, 609–623, 1981.

Dickson A. G.:Standard potential of the reaction: AgCI(s) + 1/2H2(g) = Ag(s) + HCI(aq), and the standard acidity constant of the ion HSO4 in synthetic sea water from 273.15 to 318.15 K. Journal of Chemical Thermodynamics 22, 113-127, 1990.

Dickson, A.G.: Standards for ocean measurements. Oceanography 23, 34–47, doi:10.5670/oceanog.2010.22, 2010.

Dickson, A. G., Sabine, C. L., and Christian, J. R.: Guide to best practices for ocean CO 2 measurements, PICES Special Publication, 3, 1–191, 2007.

DOE. Handbook of methods for the analysis of the various parameters of the carbon dioxide system in sea water; version 2, A. G. Dickson and C. Goyet, Eds. ORNL/CDIAC-74, 1994.

Edmond, J.M.: High precision determination of titration alkalinity and the total carbone dioxide contentof seawater by potentiometric titration. Deep Sea Res., 17, 737-750, 1970.

Feely, R.A., Sabine, C.L. , Lee, K. , Berelson, W., Kleypas, J., Fabry, V.J. , and Millero, F.J.: Impact of anthropogenic CO2 on the CaCO3 system in the oceans. Science 305(5682):362–366, doi:10.1126/science.1097329, 2004.

Fumenia, A., Moutin, T., Bonnet, S., Benavides, M., Petrenko, A., Helias Nunige, S., and Maes, C.: Excess nitrogen as a marker of intense dinitrogen fixation in the Western Tropical South Pacific Ocean: impact on the thermocline waters of the South Pacific, Biogeosciences Discuss., https://doi.org/10.5194/bg-2017-557, in review, 2018.

Ganachaud, A., et al.: The Solomon Sea: its circulation, chemistry, geochemistry and biology explored during two oceanographic cruises Elem Sci Anth, 5: 33, doi: https://doi.org/10.1525/elementa.221, 2017.

Garcia, H.E., and Gordon, L.I.: Oxygen solubility in seawater: Better fitting equations. Limnol. Oceanogr. 37:1307-1312, doi:10.4319, 1992.

Gattuso, J.-P. and Lavigne, H.: Technical Note: Approaches and software tools to investigate the impact of ocean acidification, Biogeosciences, 6, 2121-2133, https://doi.org/10.5194/bg-6-2121-2009, 2009.

Gruber, N. and Sarmiento, J.L.: Global patterns of marine nitrogen fixation and denitrification, Global Biogeochemical Cycles, 655 11, 2, 235 -266, 1997.

Hartin, C.A., Fine, R.A., Sloyan, B.M., Talley, L.D., Chereskin, T.K. and Happell, J. : Formation rates of Subantarctic mode water and Antarctic intermediate water within the South Pacific. Deep-Sea Research Part I: Oceanographic Research Papers, 58(5), 524-534. DOI: 10.1016/j.dsr.2011.02.010, 2011.

Khatiwala, S., Tanhua, T., Mikaloff, T., Fletcher, S., Gerber, M., Doney, S. C., Graven, H. D., Gruber, N., McKinley, G. A., Murata, A., Ríos, A. F. and Sabine, C. L.: Global ocean storage of anthropogenic carbon, Biogeosciences, 10, 2169-2191, https://doi.org/10.5194/bg-10-2169-2013, 2013.

Key, R. M., Kozyr A., Sabine C.L., Lee K., Wanninkhof R., Bullister J. L., Feely R. A.,Millero F. J., Mordy C., and Peng T.-H.: A global ocean carbon climatology: Results from Global Data Analysis Project (GLODAP), Global Biogeochem. Cycles, 18, GB4031, doi:10.1029/2004GB002247, 2004.

Kouketsu, S., Murata, A. and Doi T.: Decadal changes in dissolved inorganic carbon in the Pacific Ocean, Global Biogeochem. Cycles, 27, 65–76, doi:10.1029/2012GB004413, 2013.

Langdon, C.: Determination of Dissolved Oxygen in Seawater by Winkler Titration Using the Amperometric Technique In The GO-SHIP Repeat Hydrography Manual: A Collection of Expert Reports and Guidelines. Hood, E.M., C.L. Sabine, and B.M. Sloyan, eds. IOCCP Report Number 14, ICPO Publication Series Number 134. Available online at: http://www.go-ship.org/HydroMan.html, 2010.

Lauvset, S. K., Gruber, N., Landschützer, P., Olsen, A., and Tjiputra, J.: Trends and drivers in global surface ocean pH over the past 3 decades, Biogeosciences, 12, 1285–1298, doi:10.5194/bg-12-1285-2015, 2015.

Le Quéré, C., Andrew, R. M., Friedlingstein, P., Sitch, S., Pongratz, J., Manning, A. C., Korsbakken, J. I., Peters, G. P., Canadell, J. G., Jackson, R. B., Boden, T. A., Tans, P. P., Andrews, O. D., Arora, V. K., Bakker, D. C. E., Barbero, L., Becker, M., Betts, R. A., Bopp, L., Chevallier, F., Chini, L. P., Ciais, P., Cosca, C. E., Cross, J., Currie, K., Gasser, T., Harris, I., Hauck, J., Haverd, V., Houghton, R. A., Hunt, C. W., Hurtt, G., Ilyina, T., Jain, A. K., Kato, E., Kautz, M., Keeling, R. F., Klein Goldewijk, K., Körtzinger, A., Landschützer, P., Lefèvre, N., Lenton, A., Lienert, S., Lima, I., Lombardozzi, D., Metzl, N., Millero, F., Monteiro, P. M. S., Munro, D. R., Nabel, J. E. M. S., Nakaoka, S.-I., Nojiri, Y., Padin, X. A., Peregon, A.,

Pfeil, B., Pierrot, D., Poulter, B., Rehder, G., Reimer, J., Rödenbeck, C., Schwinger, J., Séférian, R., Skjelvan, I., Stocker, B. D., Tian, H., Tilbrook, B., Tubiello, F. N., van der Laan-Luijkx, I. T., van der Werf, G. R., van Heuven, S., Viovy, N., Vuichard, N., Walker, A. P., Watson, A. J., Wiltshire, A. J., Zaehle, S., and Zhu, D.: Global Carbon Budget 2017, Earth Syst. Sci. Data, 10, 405-448, https://doi.org/10.5194/essd-10-405-2018, 2018.

Lo Monaco C., Goyet, C., Metzl, N., Poisson, A., and Touratier, F.: Distribution and inventory of anthropogenic CO 2 in the Southern Ocean: comparison of three data-based methods, J. Geophs. Res., 110, C09S02, doi:10.1029/2004JC002571, 2005.

Lueker, T. J., Dickson, A., and Keeling, C. D.: Ocean pCO 2 calculated from dissolved inorganic carbon, alkalinity, and equations for K1 and K2: validation based on laboratory measurements of CO 2 in gas and seawater at equilibrium, Mar. Chem., 70(1–3), 105–119, 2000.

Moutin, T., Doglioli, A. M., de Verneil, A., and Bonnet, S.: Preface: The Oligotrophy to the UlTra-oligotrophy PACific Experiment (OUTPACE cruise, 18 February to 3 April 2015), Biogeosciences, 14, 3207-3220, https://doi.org/10.5194/bg-14-3207-2017, 2017.

Moutin, T., Wagener, T., Caffin, M., Fumenia, A., Gimenez, A., Baklouti, M., Bouruet-Aubertot, P., Pujo-Pay, M., Leblanc, K., Lefevre, D., Helias Nunige, S., Leblond, N., Grosso, O., and de Verneil, A.: Nutrient availability and the ultimate control of the biological carbon pump in the Western Tropical South Pacific Ocean, Biogeosciences Discuss., https://doi.org/10.5194/bg-2017-565, in review, 2018.

Murata, A., Kumamoto Y., Watanabe S., and Fukasawa M.: Decadal increases of anthropogenic CO2 in the South Pacific subtropical ocean along 32°S, J. Geophys. Res., 112 , C05033, doi:10.1029/2005JC003405, 2007.

Murata, A., Hayashi, K., Kumamoto, Y. and Sasaki, K.:Detecting the progression of ocean acidification from the saturation state of $CaCO_3$ in the subtropical South Pacific, Global Biogeochem. Cycles, 29, 463–475, doi:10.1002/2014GB004908, 2015.

Olsen, A., Key, R. M., van Heuven, S., Lauvset, S. K., Velo, A., Lin, X., Schirnick, C., Kozyr, A., Tanhua, T., Hoppema, M., Jutterström, S., Steinfeldt, R., Jeansson, E., Ishii, M., Pérez, F. F., and Suzuki, T.: The Global Ocean Data Analysis Project version 2 (GLODAPv2) – an internally consistent data product for the world ocean, Earth Syst. Sci. Data, 8, 297-323, https://doi.org/10.5194/essd-8-297-2016, 2016.

Oudot, C., Gerard, R., Morin, P., Gningue, I..: Precise shipboard determination of dissolved-oxygen (Winkler Procedure) with a commercial system. Limnol. Oceanogr., 33, 1, 146-150, WOS:A1988M521700015, 1988.

Owens, W.B., and Millard Jr., R.C.: A new algorithm for CTD oxygen calibration. J. Phys. Oceanogr., 15, 621-631, 1985.

Perez, F. F. and Fraga, F.: A precise and rapid analytical procedure for alkalinity determination, Mar. Chem., 21, 169–182, 1987.

Raven, J., et al.: Ocean Acidification due to Increasing Atmospheric Carbon Dioxide. The Royal Society, London, 59 pp, 2005

Riebesell, U., Zondervan, I., Rost, B., Tortell, P.D., Zeebe, R.E. and Morel, F.M.M.: Reduced calcification of marine plankton in response to increased atmospheric CO_2. Nature. 407(6802): 364–7. doi: 10.1038/35030078, 2000.

Sabine, C. L., R. A. Feely, R. M. Key, J. L. Bullister, F. J. Millero, K. Lee, T.-H. Peng, B. Tilbrook, T. Ono, and C. S. Wong: Distribution of anthropogenic CO_2 in the Pacific Ocean, Global Biogeochem. Cycles, 16(4), 1083, doi:10.1029/2001GB001639, 2002.

Sabine, C. L., Feely, R. A., Gruber, N., Key, R. M., Lee, K., Bullister, J. L., Wanninkhof, R., Wong, C. S., Wallace, D. W. R., Tilbrook, B., Millero, F. J., Peng, T.-H., Kozyr, A., Ono, T., and Rios, A. F.: The oceanic sink for anthropogenic CO_2 , Science, 305, 367–371, 2004.

Sabine, C. L., Feely, R.A., Millero, F. J., Dickson, A.G., Langdon, C., Mecking, S. and Greeley, D.: Decadal Changes in Pacific Carbon. Journal of Geophysical Research , 113 , C07021, doi: 10.1 029/2007JC004577, 2008.

Sabine, C.L. and Tanhua, T.: Estimation of Anthropogenic CO_2 Inventories in the Ocean, Annual Reviews of Marine Science, 2, 269-92. doi:10.1146/annurev-marine-120308-080947, 2010.

Takahashi, T., Sutherland, S. C., Chipman, D. W., Goddard, J. G., Cheng Ho, Newberger, T., Sweeney, C., Munro, D. R.: Climatological Distributions of pH, pCO_2 , Total CO2 , Alkalinity, and CaCO3 Saturation in the Global Surface Ocean, and Temporal Changes at Selected Locations. Mar. Chem. doi: 10.1016/j.jmarchem.2014.06.004, 2014.

Tomczak, M., and J. S. Godfrey: Regional oceanography: An introduction, pdf version 1.0. [Available at http://www.esflinders.edu.au/~mattom/regoc/pdfversion.html], 2001.

Touratier, F. and Goyet, C.: Definition, properties, and Atlantic Ocean distribution of the new tracer TrOCA, J. Mar. Sys., 46, 169–179, 2004a.

Touratier, F. and Goyet, C.: Applying the new TrOCA approach to assess the distribution of anthropogenic CO2 in the Atlantic Ocean, J. Mar. Sys., 46, 181–197, 2004b.

Touratier, F., Azouzi, L., and Goyet, C.: CFC-11, $\Delta^{14}C$ and ^{3}H tracers as a means to assess anthropogenic CO2 concentrations in the ocean, Tellus B, 59, 318–325, 2007.

Valladares, J., Fennel, W., Morozov,E.G.: Anouncement: Replacement of EOS-80 with the International Thermodynamic Equation of Seawater—2010 (TEOS-10). Deep Sea Research, 58, 978, doi:10.1016/j.dsr.2011.07.005, 2011.

Vázquez-Rodríguez, M., Touratier, F., Lo Monaco, C., Waugh, D. W., Padin, X. A., Bellerby, R. G. J., Goyet, C., Metzl, N., Ríos, A. F., and Pérez, F. F.: Anthropogenic carbon distributions in the Atlantic Ocean: data-based estimates from the Arctic to the Antarctic, Biogeosciences, 6, 439-451, https://doi.org/10.5194/bg-6-439-2009, 2009.

Waters, J.F., Millero F. J. and Sabine C.L.: Changes in South Pacific anthropogenic carbon, Global Biogeochem. Cycles, 25(4), GB4011, doi:10.1029/2010GB003988, 2011.

Winkler, L. W.: Die Bestimmung des im Wasser gelosten Sauerstoffes. Ber. Dtsch. Chem. Ges. 21: 2843-2853, 1888.

Yool, A., Oschlies, A., Nurser, A. J. G., and Gruber, N.: A model-based assessment of the TrOCA approach for estimating anthropogenic carbon in the ocean, Biogeosciences, 7, 723-751, https://doi.org/10.5194/bg-7-723-2010, 2010.

Yoshikawa, C., Makabe, A., Shiozaki, T., Toyoda, S., Yoshida, O., Furuya, K., and Yoshida. N.: Nitr
ogen isotope ratios of nitrate and N* anomalies in the subtropical South Pacic, Geochemistry Geophysics, Geosystem, 16, 1439– 1448, 2015

Biogeosciences Discuss., https://doi.org/10.5194/bg-2018-163
Manuscript under review for journal Biogeosciences
Discussion started: 17 April 2018

Table 1 : General description of the cast sampled for carbonate chemistry parameters during the OUTPACE cruise.

Cast	Station	Longitude (°E)	Latitude (°N)	Time (UTC)	Max Pres.	Type*	Rosette**
out_c_006	SD 1	159,9255	-17,9418	2015/02/22 03:08:00	202	SHAW	CLA
out_t_002		159,9425	-17,9088	2015/02/22 07:43:00	2000	INT	TMC
out_c_010	SD 2	162,1248	-18,6078	2015/02/23 00:11:00	199	SHAW	CLA
out_c_016		162,1112	-18,5845	2015/02/23 08:16:00	1998	INT	CLA
out_c_019	SD 3	165,0093	-19,4955	2015/02/24 05:58:00	200	SHAW	CLA
out_c_020		165,0082	-19,4907	2015/02/24 08:14:00	1999	INT	CLA
out_c_066	LD A	164,5877	-19,2242	2015/03/02 14:39:00	200	SHAW	CLA
out_c_067		164,5787	-19,2233	2015/03/02 16:10:00	2002	INT	CLA
out_c_070	SD 4	168,0118	-19,9832	2015/03/04 10:55:00	201	SHAW	CLA
out_c_071		168,0157	-19,98	2015/03/04 12:43:00	1999	INT	CLA
out_c_074	SD5	169,9943	-22,0002	2015/03/05 08:48:00	201	SHAW	CLA
out_c_075		169,9965	-21,9997	2015/03/05 10:27:00	1999	INT	CLA
out_c_078	SD6	172,1198	-21,3732	2015/03/06 07:27:00	200	SHAW	CLA
out_c_079		172,1193	-21,3758	2015/03/06 09:08:00	1999	INT	CLA
out_c_082	SD7	174,25	-20,7697	2015/03/07 05:09:00	201	SHAW	CLA
out_c_083		174,2512	-20,7677	2015/03/07 06:37:00	2000	INT	CLA
out_c_086	SD8	176,3778	-20,7027	2015/03/08 02:31:00	201	SHAW	CLA
out_c_087		176,364	-20,6945	2015/03/08 04:19:00	1997	INT	CLA
out_c_091	SD9	178,6087	-20,9963	2015/03/09 04:57:00	2002	INT	CLA
out_t_012		178,6062	-20,9892	2015/03/09 06:46:00	201	SHAW	TMC
out_c_094	SD10	-178,5105	-20,4417	2015/03/10 04:10:00	200	SHAW	CLA
out_c_095		-178,5105	-20,44	2015/03/10 05:48:00	762	INT	CLA
out_c_098	SD11	-175,6542	-20,0028	2015/03/11 00:53:00	207	SHAW	CLA
out_c_099		-175,6475	-20,0057	2015/03/11 02:46:00	2000	INT	CLA
out_c_102	SD12	-172,7885	-19,5237	2015/03/12 00:38:00	200	SHAW	CLA
out_c_103		-172,7813	-19,5368	2015/03/12 02:26:00	2001	INT	CLA
out_c_150	B	-170,7433	-18,179	2015/03/20 12:38:00	204	SHAW	CLA
out_c_151		-170,7385	-18,1745	2015/03/20 14:16:00	1997	INT	CLA
out_c_152	SD13	-169,0728	-18,2007	2015/03/21 10:27:00	501	INT	CLA
out_c_163	C	-165,9315	-18,4282	2015/03/24 12:23:00	5027	DEEP	CLA
out_c_194		-165,8647	-18,4952	2015/03/28 02:01:00	25	REPRO	CLA
out_c_198		-165,7915	-18,4912	2015/03/28 12:42:00	298	SHAW	CLA
out_c_199		-165,7792	-18,4842	2015/03/28 14:32:00	2001	INT	CLA
out_c_209	SD14	-163,001	-18,395	2015/03/30 05:19:00	300	SHAW	CLA
out_c_210		-162,9992	-18,3952	2015/03/30 07:03:00	2000	INT	CLA
out_c_212	SD15	-159,9913	-18,265	2015/03/31 04:01:00	300	SHAW	CLA
out_c_213		-159,9913	-18,2618	2015/03/31 05:41:00	2002	INT	CLA

*: SHAW stands for casts up to 200 dbar, INT stands for casts up to 2000m, DEEP stands for the deep cast and REPRO stands for the cast with reproducibility measurements

Biogeosciences Discuss., https://doi.org/10.5194/bg-2018-163
Manuscript under review for journal Biogeosciences
Discussion started: 17 April 2018

**: CTD rosette used for the cast. CLA is the normal CTD rosette and TMC is the trace metal clean rosette (See Sect. 2.1)

Biogeosciences Discuss., https://doi.org/10.5194/bg-2018-163
Manuscript under review for journal Biogeosciences
Discussion started: 17 April 2018

Table 2 : Estimated inventories of C_{ANT} up to 1000 and 2000 meters (see text for details) and estimated depth of the $\Omega_{ara} = 1$ horizon along the OUTPACE cruise (see text for details). No values are available for stations where data up to 2000 dbar were not available (SD2 and SD13). For the depth of the $\Omega_{ara} = 1$ horizon , no values were estimated for stations with $C_{ANT} < -6$ µmol kg^{-1}.

Station	Longitude	Latitude	Inventory for C_{ANT} ($mol.m^{-2}$)			Depth of the $\Omega_{ara} = 1$ horizon (in m)		
			$C_{ANT}INV_{2000}$	$C_{ANT}INV_{1000}$	% in 1000m*	OUTPACE	Pre-indu.	Difference**
SD1	159,9425	-17,9088	43	38,6	89,7	1225	NA	NA
SD2	162,1248	-18,6078	NA	NA	NA	NA	NA	NA
SD3	165,0082	-19,4907	44,8	39,6	88,3	928	NA	NA
A	164,5787	-19,2233	39,7	35,2	88,6	1032	1185	153
SD4	168,0157	-19,98	43,7	36,2	82,8	1029	1193	164
SD5	169,9965	-21,9997	49,4	41,2	83,4	1126	1256	130
SD6	172,1193	-21,3758	47	41,2	87,6	1097	1233	136
SD7	174,2512	-20,7677	44,6	36,7	82,2	1015	1235	220
SD8	176,364	-20,6945	42,7	38,3	89,6	1010	1171	161
SD9	178,6087	-20,9963	36,6	34,8	95,1	1214	NA	NA
SD11	-175,6475	-20,0057	37,2	34,1	91,6	1055	1172	117
SD12	-172,7813	-19,5368	39,7	37,4	94,2	1013	1112	99
B	-170,7385	-18,1745	36	34,5	95,8	948	1046	98
SD13	-169,0728	-18,2007	NA	NA	NA	NA	NA	NA
C	-165,7792	-18,4842	37,7	36,1	95,7	854	941	87
SD14	-162,9992	-18,3952	37,3	34,4	92,2	889	1006	117
SD15	-159,9913	-18,2618	36,9	35,3	95,6	917	1043	126

***** Percentage of $C_{ANT}INV_{2000}$ estimated in $C_{ANT}INV_{1000}$

** Difference (in m) between the depth of the $\Omega_{ara} = 1$ horizon at the pre-industrial period and the OUTPACE cruise.

Biogeosciences Discuss., https://doi.org/10.5194/bg-2018-163
Manuscript under review for journal Biogeosciences
Discussion started: 17 April 2018

Table 3 : Estimated trends on A_T, $[O_2]$, C_T , C_{ANT} and pH_T changes in two different layers of the water column defined by isopycnal layers between 1980 and 2015 based on GLODAPv2 and OUTPACE. Estimated trends are obtained from slope values of a linear regression between the studied parameters and time.

	$25 < \sigma_\theta < 25.5$	$27 < \sigma_\theta < 27.2$
	Trend on A_T	
OUTPACE area	-0.20 ± 0,07 µmol.kg^{-1}.a^{-1} (n = 167) *	-0.12 ± 0,07 µmol.kg^{-1}.a^{-1} (n = 180)
MA area	-0.30 ± 0.09 µmol.kg^{-1}.a^{-1} (n = 85) *	-0.16 ± 0.09 µmol.kg^{-1}.a^{-1} (n = 99)
WGY area	-0,20 ± 0.14 µmol.kg^{-1}.a^{-1} (n = 28)	-0,20 ± 0.14 µmol.kg^{-1}.a^{-1} (n = 35)
	Trend on $[O_2]$	
OUTPACE area	-0.31 ± 0.10 µmol.kg^{-1}.a^{-1} (n = 167)	0.05 ± 0.11 µmol.kg^{-1}.a^{-1} (n = 183)
MA area	-0.35 ± 0.16 µmol.kg^{-1}.a^{-1} (n = 84)	0.06 ± 0.11 µmol.kg^{-1}.a^{-1} (n = 99)
WGY area	-0.38 ± 0.11 µmol.kg^{-1}.a^{-1} (n = 27)	-0,11 ± 0.30 µmol.kg^{-1}.a^{-1} (n = 38)
	Trend on C_T	
OUTPACE area	1.32 ± 0.13 µmol.kg^{-1}.a^{-1} (n = 174) *	0.23 ± 0.13 µmol.kg^{-1}.a^{-1} (n = 189)
MA area	1.38 ± 0.21 µmol.kg^{-1}.a^{-1} (n = 85) *	0.31 ± 0.16 µmol.kg^{-1}.a^{-1} (n = 100)
WGY area	1.57 ± 0.18 µmol.kg^{-1}.a^{-1} (n = 31) *	0.23 ± 0.29 µmol.kg^{-1}.a^{-1} (n = 40)
	Trend on C_{ANT}	
OUTPACE area	1.12 ± 0.07 µmol.kg^{-1}.a^{-1} (n = 166) *	0.32 ± 0.05 µmol.kg^{-1}.a^{-1} (n = 179) *
MA area	1.18 ± 0.08 µmol.kg^{-1}.a^{-1} (n = 84) *	0.40 ± 0.06 µmol.kg^{-1}.a^{-1} (n = 98) *
WGY area	1.20 ± 0.09 µmol.kg^{-1}.a^{-1} (n = 28) *	0.13 ± 0.09 µmol.kg^{-1}.a^{-1} (n = 35)
	Trend on pH_{TINSI}	
OUTPACE area	-0.0022 ± 0.0003 a^{-1} (n=167) *	-0.0001 ± 0.0003 a^{-1} (n=181)
MA area	-0.0022 ± 0.0004 a^{-1} (n = 85) *	-0.0004 ± 0.0003 a^{-1} (n=100)
WGY area	-0.0027 ± 0.0004 a^{-1} (n = 28) *	-0.00008 ± 0.0006 a^{-1} (n=35)

* : trend significant (p-level < 0.05)

Biogeosciences Discuss., https://doi.org/10.5194/bg-2018-163
Manuscript under review for journal Biogeosciences
Discussion started: 17 April 2018

Figures

Fig. 1: Map of the OUTPACE cruise transect. The outpace stations are distinguished between Melanesian Archipelago (MA) stations with darkgreen large dots and the Western GYre (WGY) stations with dark blue large dots. Stations outside of these two areas are in grey. The station with a red indication corresponds to the station where the deep cast and intercomparaison cast was made. Station from the GLODAPv2 database are indicated with small dots: small green dots correspond to GLODAPv2 stations considered for comparaison in the MA area, small blue dots correspond to GLODAPv2 stations considered for comparaison in the WGY area and small grey dots are the other stations.

Fig. 2: $\Theta - S_A$ diagram with colors indicating the AOU. Black contour lines represent the isopycnal horizons based on potential density referenced to a pressure of 0 dBar (σ_θ).

Fig. 3: Longitudinal variations of (a) A_T, (b) C_T, (c) pH_T and (d) Ω_{ara} along the OUTPACE transect between surface and 2000m depth. Black contour lines represent the isopycnal horizons based on potential density referenced to a pressure of 0 dBar. Vertical profiles of (e) A_T, (f) A_T normalized to SA =35 and (g) C_T of the entire OUTPACE dataset (red dots) superimposed on the GLODAPv2 data corresponding to the OUTPACE area (grey dots).

Fig. 4: Longitudinal variations C_{ANT} (Estimated with the TROCA method) along the OUTPACE transect between surface and 2000m depth (a). Black contour lines represents the isopycnal horizons based on potential density referenced to a pressure of 0 dBar. Vertical profiles of C_{ANT} for the entire OUTPACE dataset superimposed on the values estimated from the GLODAPv2 data (b) and vertical profiles of of C_{ANT} between surface and 1500m superimposed on the values estimated from the recent (after 2005) GLODAPv2 data (c). Color code for the dots is the same as for Figure 1

Fig. 5: Temporal evolution in the OUTPACE area of C_T (a and c), C_{ANT} (b and d) and pH_{Tinsi} (c and e) based on GLODAPv2 and OUTPACE data along two isopycnal layers: 25 – 25.5 $kg.m^{-3}$ (left side panels) and 27 - 27.2 $kg.m^{-3}$ (right side panels). Color code for the dots is the same as for Figure 1.

Fig. 6: Longitudinal variations of (a) pH_T changes and (b) Ω_{ara} changes between pre-industrial and present time along the OUTPACE transect between surface and 2000m depth (See text for details). Black contour lines represent the isopycnal horizons based on potential density referenced to a pressure of 0 dBar. Panel (c) represents longitudinal variations of inventories of C_{ANT} ($C_{ANT}INV_{2000}$) plotted in grey (see table 2 for details) and the depth of the $\Omega_{ara} = 1$ horizon (in m) during OUTPACE (red dots) and at the pre-industrial period (Black dots). The red area illsutrates the shoaling of the $\Omega_{ara} = 1$ horizon since the pre-industrial period.

Biogeosciences Discuss., https://doi.org/10.5194/bg-2018-163
Manuscript under review for journal Biogeosciences
Discussion started: 17 April 2018

Fig. 1

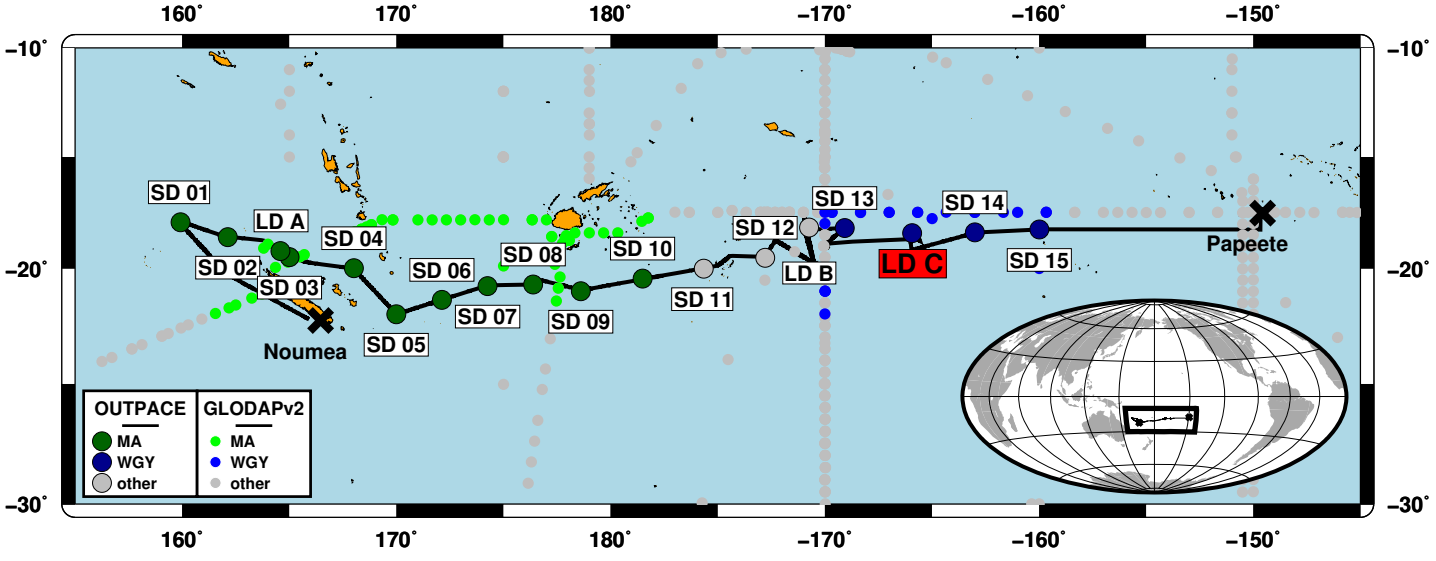

Biogeosciences Discuss., https://doi.org/10.5194/bg-2018-163
Manuscript under review for journal Biogeosciences
Discussion started: 17 April 2018

Fig. 2

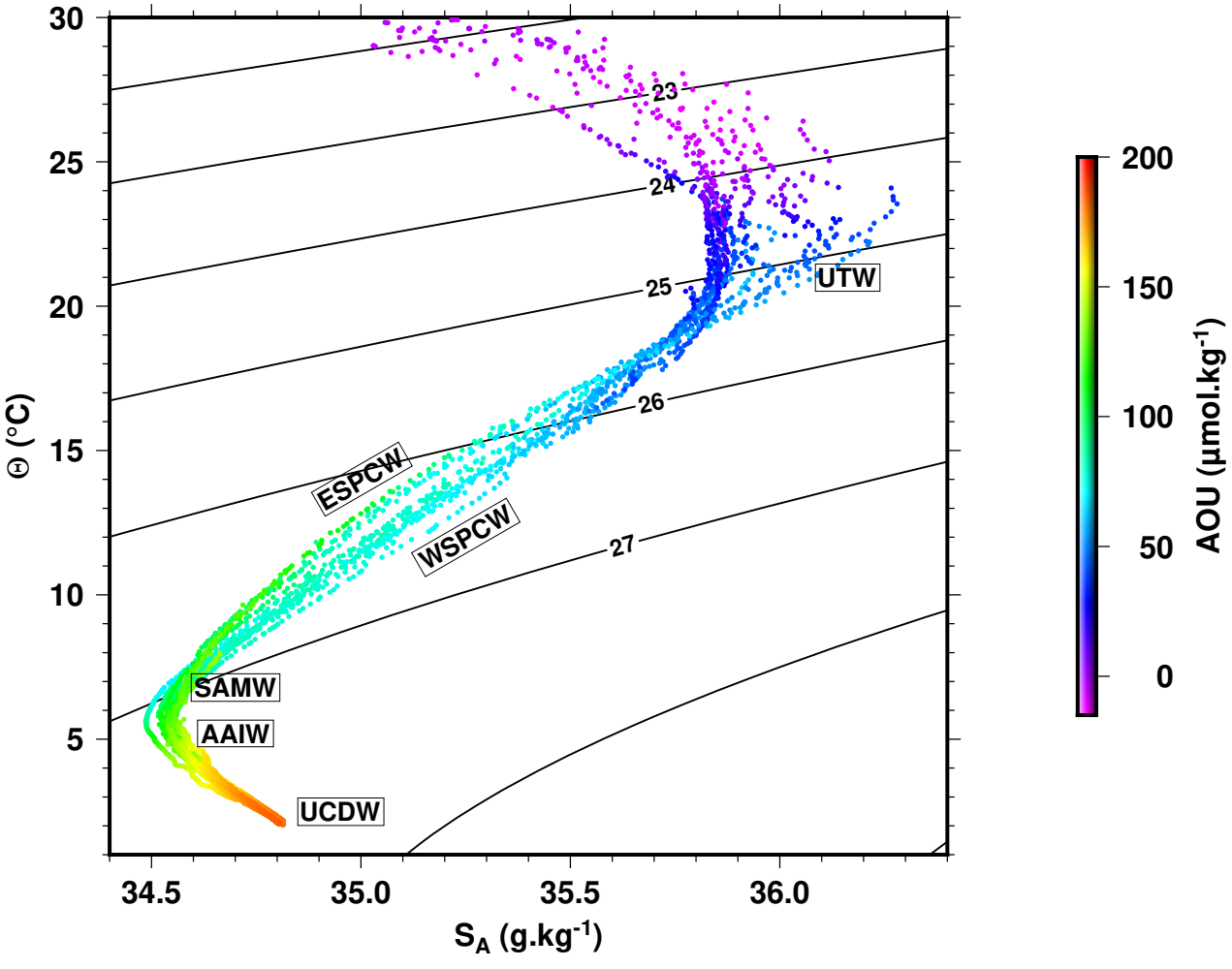

Biogeosciences Discuss., https://doi.org/10.5194/bg-2018-163
Manuscript under review for journal Biogeosciences
Discussion started: 17 April 2018

590 Fig. 3

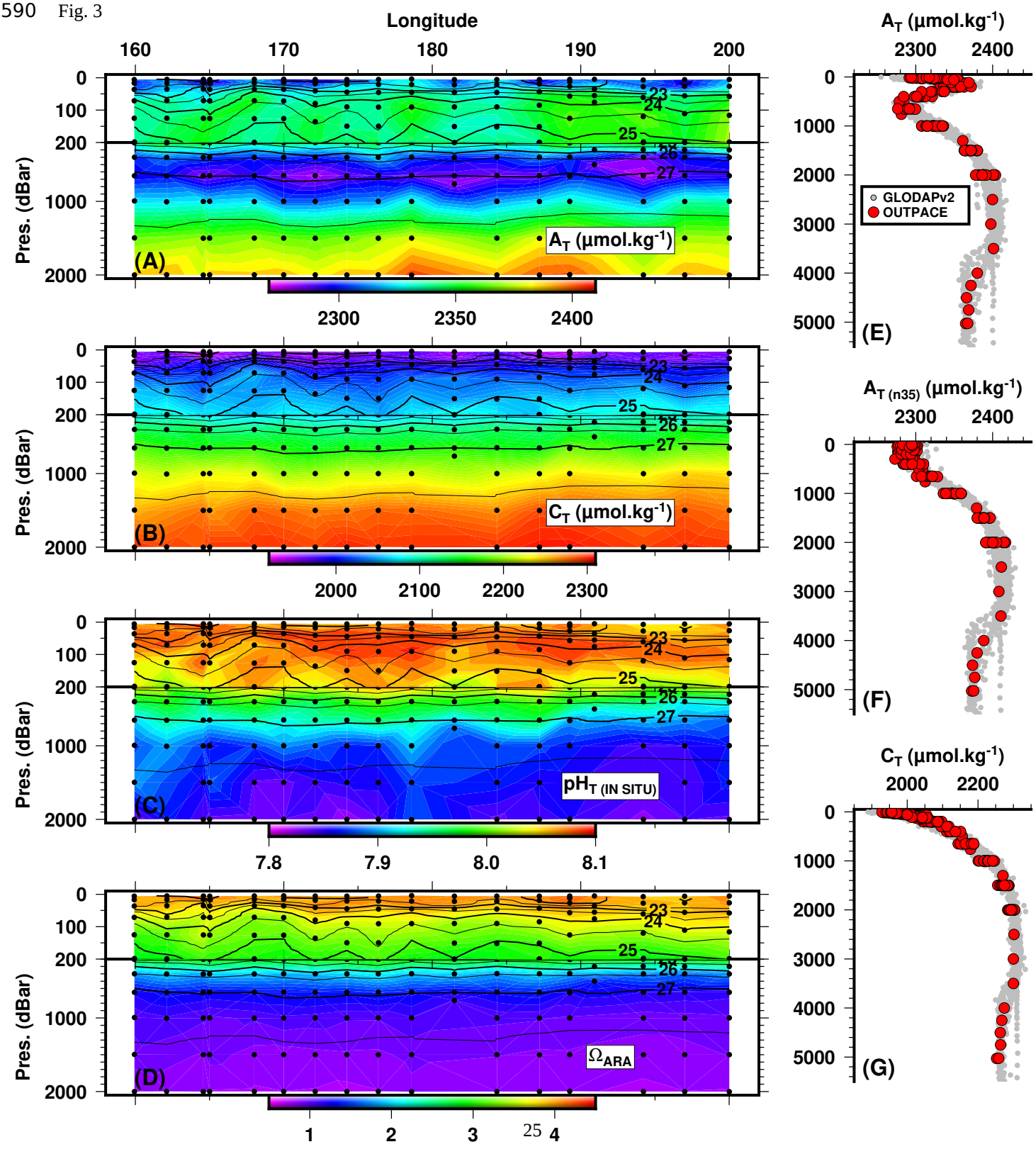

Biogeosciences Discuss., https://doi.org/10.5194/bg-2018-163
Manuscript under review for journal Biogeosciences
Discussion started: 17 April 2018

Fig. 4

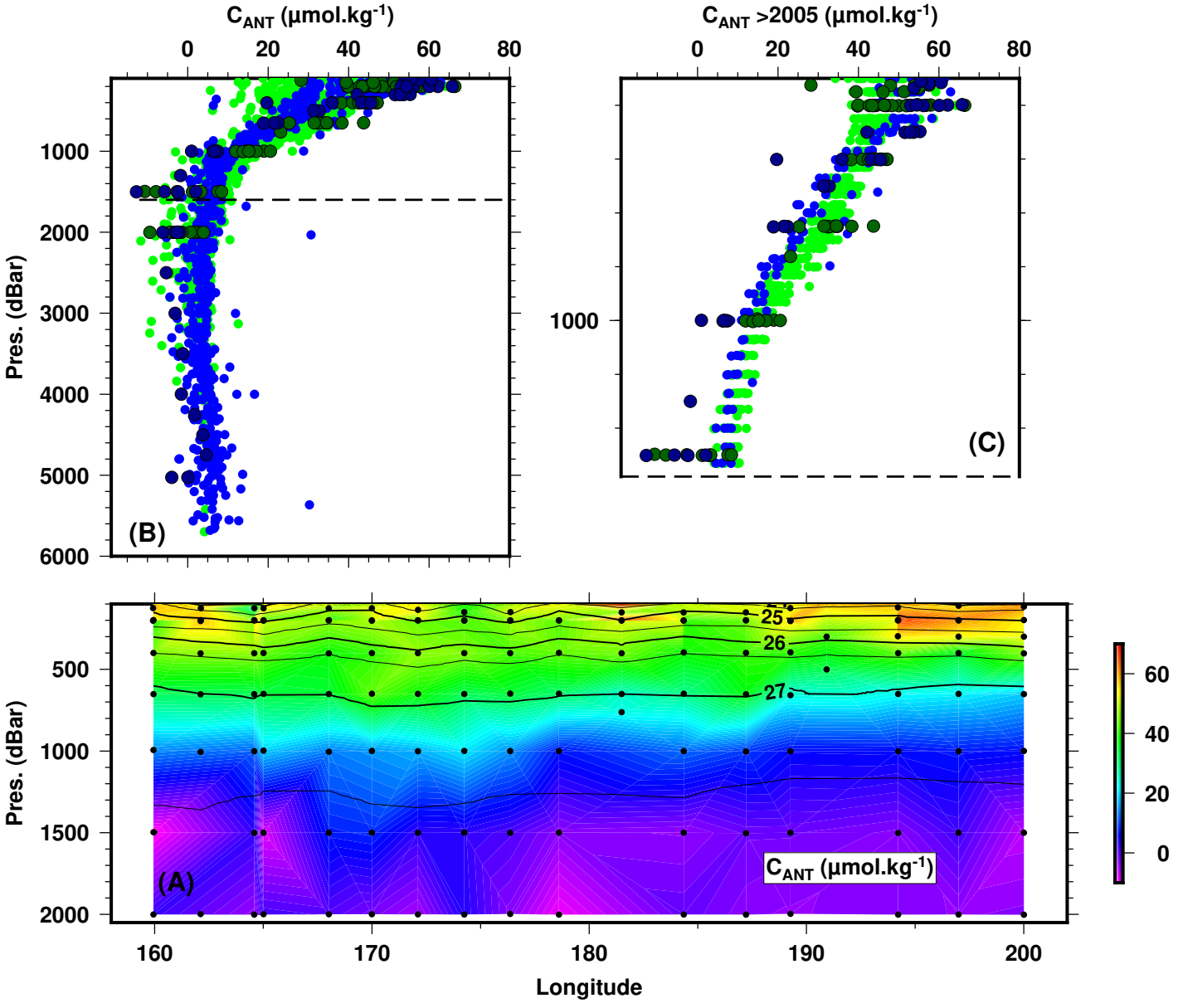

Biogeosciences Discuss., https://doi.org/10.5194/bg-2018-163
Manuscript under review for journal Biogeosciences
Discussion started: 17 April 2018

Fig. 5

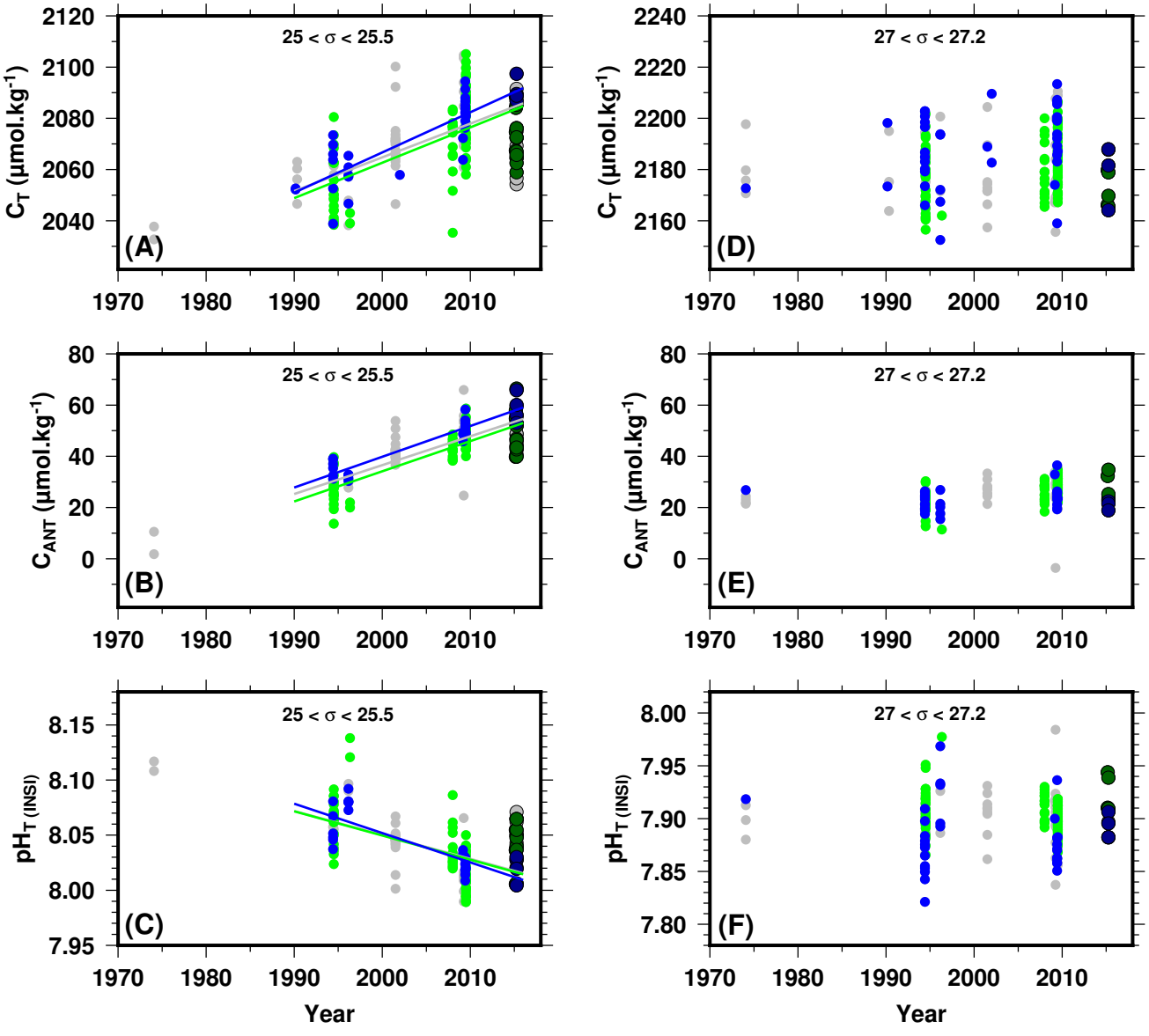

Biogeosciences Discuss., https://doi.org/10.5194/bg-2018-163
Manuscript under review for journal Biogeosciences
Discussion started: 17 April 2018

Fig. 6